LIMITATIONS ON TRANSMUTATION PERFORMANCE DUE TO REACTIVITY CONSTRAINTS IN ACCELERATOR DRIVEN SYSTEMS

José M. Martínez-Val, J.Manuel Perlado, Emilio Mínguez, Mireia Piera, Akinori Oda
E.T.S.I.I.-U.P.M., J. Gutiérrez Abascal, 2, Madrid 28006,
Spain

Abstract

An analysis is presented to characterise the reactivity effects in molten lead energy amplifiers. Limitations in the nominal k-eff value to avoid reaching criticality in abnormal conditions impose restrictions to the nominal value of the neutron flux. If those restrictions become very severe because of safety features, the transmutation performance would not be good enough. Very long burnup periods would be needed to reach a certain level of transmutation cleansing.

Introduction

Transmutation of transuranics into shorter-living nuclei is possible by nuclear fission. In fact, it produces a near-term amplification of radioactivity, because fission products convey about ten decays per fission before reaching nuclear stability, and those decays happen in a period shorter than 400 years. On the contrary, a transuranic nucleus will also go through ten decays (in rough numbers) before arriving to a stable isotope of lead, but it will take tens of thousand years to arrive to stability.

A critical point to reduce the TRU inventory is to minimise the capture cross section in relation to the fission cross section. Otherwise, higher-A actinides would appear and it would imply longer decay periods to reach stability. This criterion can be met either with very fast neutron spectra or well moderated spectra. The region of cross section resonance must particularly be avoided.

A second fundamental point in this context is to have a high transmutation rate, and this means a high $\sigma\phi$ value. In thermal reactors, σ is very large, but ϕ is small for a given neutron concentration density (N) because the neutron speed is low. On the contrary, σ is small in fast spectra, but ϕ can be much higher. Anyway, if a substantial fraction of a given inventory has to be transmuted in a given time, the value $\sigma\phi$ must reach a certain value.

The flux level is also connected with the power density in the reactor

$$D(W/m^3) = a\sum \sigma_f^i \phi N_i$$

where the summatory applies to all fissionable isotopes and *a* is a constant for unit change. For the sake of simplicity, let us assume the reactor fuel is mainly made of ^{239}Pu. It could be written

$$D = a\sigma_f^9 \phi N^9$$

Therefore, a limit to D (because of thermal-hyudraulics) is a limit to the concentration of ^{239}Pu (N^9). Of course, if V is the volume of the reactor, it holds $^{239}Pu = V.N^9$. If N^9 has to be reduced because of thermalhydraulics reasons, the reactor volume has to be increased, for a given inventory ^{239}Pu.

In any case, a high flux is needed and this means a high value of the k_{eff} of the subcritical reactor. Otherwise, the spallation source strength would have to be so high that the system would be unfeasible.

On the other hand, the reactor should not attain criticality in any condition, even under accidental circumstances. This means that a large enough margin of reactivity has to be accepted in the nominal design, to have room enough to accommodate the reactivity effect of any abnormal performance.

In the following, an analysis is made on the general features of molten-lead energy amplifiers (MLEA) [1-3], starting from an analytical approach to characterise in a systematic way the main reactivity effects.

Reactivity variations in a MLEA

Figure 1 presents the evolution of k_{eff} (in a lattice cell calculation) as the cell pitch changes. It must be noted that this calculation implies an infinite array of cells in the horizontal plane. In a realistic design, the fuel mass must be kept constant when changing the geometry, which means that a compacted reactor will have a smaller radius and therefore higher leakage probability.

Compactation simulations must also take into account the accidental filling of the central part of the reactor (where the spallation source is placed) by fuel pins displaced from the periphery inwards. As an example to illustrate this type of simulations, two bare cylindrical reactors have been calculated. The first was made of a homogeneous mixture of lead and fuel (10% ^{233}U) with a radius of 1.67 m and 1.5 m high. The k_{eff} in this case was 0.934. The second cylinder was of the same size as the previous one, but the central axial part (with a radius of 0.4 m) was only made of lead. Its k_{eff} was 0.909. If we take as reference reactor for a MLEA this reactor with k_{eff} = 0.909, it can be seen that the reactor will suffer a 3% increase in reactivity if the central part is also filled with fuel pins.

Another source of reactivity effects is the change in lead density. This is a similar problem to the one found in sodium-reactors and in over-moderated thermal reactors (as happened in the Chernobyl accident [4]. Lead neutronic properties are different from those of sodium. In fact, lead reactor spectrum is very bad for the production of higher actinides because capture to fission cross sections ratio is very small for any nuclei, as compared to the same ratios in a sodium reactor.

Figure 1 **k_{eff} vs cell pitch for a given fuel (4% ^{239}Pu, 6% ^{233}U, fuel pin radius = 0.5 cm)**

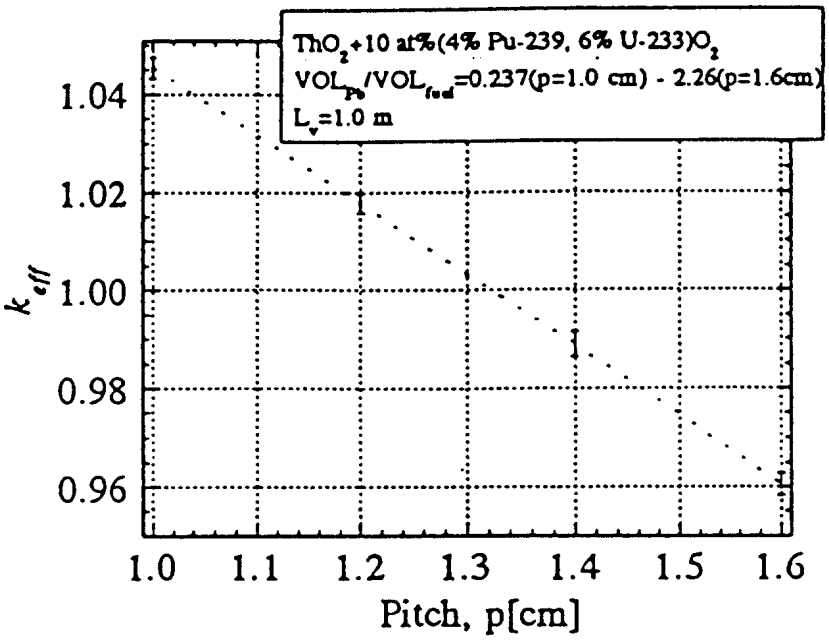

The variation of k_{eff} vs lead density is depicted in figure 2. It corresponds to a lattice cell calculations. K_{eff} remains between 0.92 and 0.96, with 0.96 at nominal density. It is important to note that the void coefficient is negative in this case, where the neutron leakage is high because we did not include in the simulation a lead reflector that can eventually remain at nominal density.

A better characterisation was analysed for selected void geometries, described as follows. A cell calculation with 2 m total height, 1.6 cm pitch and 4% ^{239}Pu plus 6% ^{233}U fissile contents was performed for four different lead distributions, which are described in the following lines, including the resulting k_{eff}:

- lead filled at reference density (10 g/cm^3) k_{eff} = 0.962
- total lead void, k_{eff} = 0.929

- central lead void (The lattice cell only simulates the upper half of the pin for symmetry reasons. In this hypothetical case, the lower half of the cell is at 0 g/cm^3 of lead, while the upper half of the lattice cell is at 10 g/cm^3) k_{eff} = 1.00
- outer void (the upper half of the lattice cell is at 0 g/cm^3 and the lower part is at 10 g/cm^3) k_{eff} = 0.917.

The foregoing results are very important because they point out that central voids produces higher reactivity effects. This is due to the harder spectrum created in the central core, where fission probability increases. This is also due to the reflector effect of the peripheral lead. On the contrary, when the void occupies outer regions, reactivity decreases because leakage of very fast neutrons is enhanced. The former physical phenomenon can further be illustrated with the calculation of another accidental scenario. In this case, it is presumed that the cladding material melts down and it goes up because of its buoyancy. Both the plenum (inside the cladding) and the cladding itself are replaced by lead. After that, it is presumed that lead density goes down (because of boiling bubbles) from nominal density (10.6 g/cm^3) to 0.0 g/cm^3. In table 1, a set of calculations of this type is presented. The reference case is a cylindrical reactor 1.2 m high plus 1.5 m plenum, with a radius of 123.6 cm and a fuel composition 86% ^{232}Th and 14% ^{239}Pu. The volume ratio Pb/fuel is 3.23 in this case. The rest of the cases in table I are denoted by the lead density in the reactor region. Outside the reactor, the lead density remains always 10.6 g/cm^3 in the whole vessel.

Figure 2 **k_{eff} vs Lead density in the standard cell calculation (4% ^{239}Pu, 6% ^{233}U)**

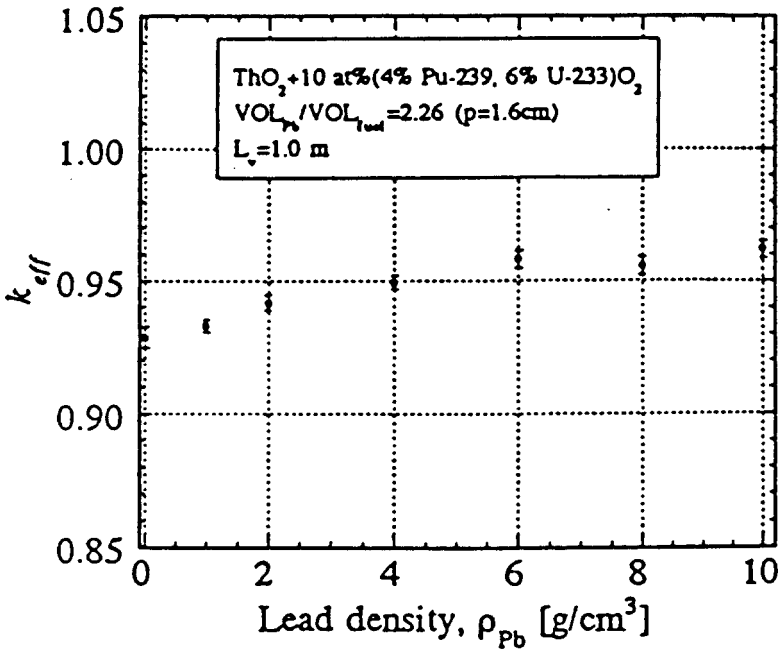

Table 1. **Reactivity injections in the case of clad melting and partial or total lead boiling**

Case (lead density g/cm^3)	k_{eff}	$\frac{\Delta k}{k}$	$\left(\frac{Fis}{Abs}\right)_f$	Abs-fuel Total Abs
Reference	0.913	0.0	0.395	0.955
10.6	0.933	0.022	0.400	0.968
9.54	0.937	0.026	0.410	0.972
6.35	0.948	0.038	0.420	0.977
2.65	0.962	0.054	0.430	0.990
1.06	0.965	0.057	0.435	0.995
0.0	0.971	0.063	0.440	1.000

Additionally, catastrophic accidents could be simulated to some extent by presuming clad melting and fuel desegregation. The fuel can go up (if it is UO_2-PuO_2)within the lead pool, and will expand laterally and shrink vertically until occupying the upper part of the vessel (below the molten clad). The results of those calculations are reported in table 2, starting from the same case of reference as table 1. Again, some increase in reactivity is found, but the lateral expansion of the (very hot) fuel prevents the reactor to achieve criticality, and the final state is highly subcritical. Of course, radioactivity confinement and emergency cooling would be the main problem in this case, but it is important to assess that the final state can not be critical.

All these calculations have been done with the LAHET [5] and MCNP [6] codes. Neutron cross-sections have been taken from ENDF B/IV [7] and ENDL [8] libraries. The JENDL 3.2 set [9] has also been used.

Table 2. **Reactivity effects due to fuel disassembly**

Case	Radius (cm)	Height (cm)	% of original lead	k_{eff}
Reference	123.6	120	100	0.913
I	126.3	100	85	0.946
II	140.1	70	70	0.947
III	149.6	25	10	0.954
IV	342.0	3.6	0	0.215

Summary

Reactivity analysis on potential changes of the reactor geometry and material composition will play an important role in the Safety Report of MLEA [10]. The need to keep subcriticality under any abnormal event that could be conceived from a practical point of view, imposes the need to have a large enough subcriticality margin. This means that the neutron flux will have a limited value and the transmutation rate will also be limited. In the Introduction, it was underlined the need of very high fluxes in order to get rid of the main TRU in a technological time span. In the Appendix, a theoretical analysis is presented to point out the cleansing levels that could be achieved in a MLEA, depending on the flux level. It is seen that ^{239}Pu transmutation is possible down to very low residual fractions. On the contrary, it is difficult to get low residual fractions (below 10%) for ^{240}Pu, which is mainly transmuted by conversion to ^{241}Pu. In any case, the need of a high flux level is paramount and it implies the need for k_{eff} as close to 1 as possible. This trend will be limited mainly by reactivity analysis related to accidental conditions.

Appendix

A theoretical study on Pu isotope transmutation

In the inventory of TRU and their associated radioactive progenie from spent nuclear fuel, the most important isotopes are ^{239}Pu, ^{240}Pu and ^{241}Pu. The first one is a very good fissile isotope, specially in fast spectrum. The last one is still better because it presents a very high σ_f and very low σ_c. If it is transmuted without allowing a long decay span, the amount of ^{241}Am built-up remains small, and the residual radiotoxicity of TRU can be highly decreased by eliminating the afro mentioned Pu isotopes. ^{240}Pu is not a good fissile material (and it is still worse for thermal spectra) but in fast spectrum it can be eliminated either directly or by conversion to ^{241}Pu.

In the following, the inherent burnup features of Pu isotopes transmutation are studied in an analytical approach. It is presumed that a subcritical reactor (in an ADS) provides for a flux ϕ and creates a spectrum in which the microscopic cross section for these isotopes are known. In our case, we take the following values typical of a MLEA [1].

$$\begin{array}{lll} ^{239}\text{Pu} & \sigma_a = 2.21 & \sigma_f = 1.75 \\ ^{240}\text{Pu} & \sigma_a = 0.82 & \sigma_f = 0.35 \\ ^{241}\text{Pu} & \sigma_a = 2.43 & \sigma_f = 2.43 \end{array} \qquad \text{(A.1)}$$

Conversion of ^{241}Pu into ^{242}Pu is not taken into account in the model, because it accounts for much less than 1% of the radiotoxicity. It is also assumed that the reactor is loaded (in any cycle) with the Pu discharged from LWR, which corresponds to the following inventory (per ton of initial Uranium loaded in the LWR)

$$\text{Pu}^9(0) = 5.19\ \text{kg} \qquad \text{Pu}^0(0) = 2.17\ \text{kg} \qquad \text{Pu}^1(0) = 1.03\ \text{kg} \qquad \text{(A.2)}$$

We use these figures as starting point. After each burnup cycle, the total amount of eliminated Pu is computed, and the same mass is reloaded (with the isotopic composition given above). The governing equations are:

$$\frac{d\text{Pu}^9}{dt} = -\sigma_a^9 \phi \text{Pu}^9 \qquad \text{(A.3)}$$

$$\frac{d\text{Pu}^0}{dt} = -\sigma_a^0 \phi \text{Pu}^0 + \sigma_c^9 \phi \text{Pu}^9 \qquad \text{(A.4)}$$

$$\frac{d\text{Pu}^1}{dt} = -\sigma_a^1 \phi \text{Pu}^1 + \sigma_c^0 \phi \text{Pu}^0 \qquad \text{(A.5)}$$

that can be solved analytically to find

$$\text{Pu}^9(t) = \text{Pu}^9(0) e^{-\sigma_a^9 \phi t} \qquad \text{(A.6)}$$

$$Pu^0(t) = Pu^0(0)e^{-\sigma_a^0\phi t} + Pu^9(0)\frac{\sigma_c^9}{\sigma_a^9 - \sigma_a^0}\left[e^{-\sigma_a^0\phi t} - e^{-\sigma_a^9\phi t}\right] \tag{A.7}$$

$$Pu^1(t) = Pu^1(0)e^{-\sigma_a^1\phi t} + Pu^0(0)\frac{\sigma_c^0}{\sigma_a^1 - \sigma_c^0}\left[e^{-\sigma_a^0\phi t} - e^{-\sigma_a^1\phi}\right] +$$
$$+ Pu^9(0)\sigma_c^9\sigma_c^0\left[\frac{e^{-\sigma_a^9\phi t}}{(\sigma_a^0 - \sigma_a^9)(\sigma_a^1 - \sigma_a^9)} + \frac{e^{-\sigma_a^0\phi t}}{(\sigma_a^9 - \sigma_a^0)(\sigma_a^1 - \sigma_a^0)} + \frac{e^{-\sigma_a^1\phi t}}{(\sigma_a^9 - \sigma_a^1)(\sigma_a^0 - \sigma_a^1)}\right] \tag{A.8}$$

In figure A.1, the evolution of the inventory is given for 24 cycles of 2.5×10^{23} n/cm^2 fluence every one. It is presumed that the microscopic cross sections do not change along the burnup, which is a hypotheses that can not be admitted for detailed calculations [11,12] of a given reactor in a given cycle, but is acceptable for an analytical study. It is observed in figure A.1 that an equilibrium cycle is achieved after 12 cycles. After that, the material unloaded from the ADS reactor has a composition given by the following fractions

$$^{239}Pu = 0.2735 \qquad ^{240}Pu = 0.5625 \qquad ^{241}Pu = 0.164 \tag{A.9}$$

Figure A.1 **Evolution of the Pu inventory in successive cycles of transmutations using LWR spent fuel (see text)**

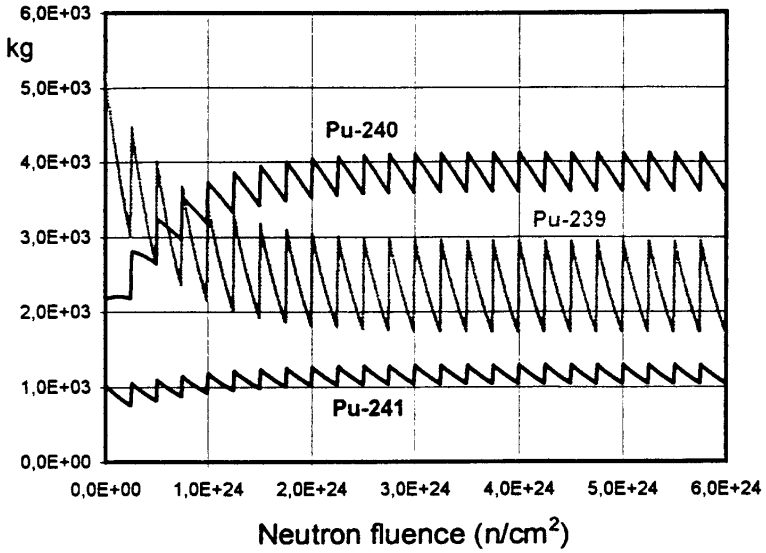

The residual fraction of each isotope is given in figure A.2. It is defined as the inventory of an isotope still existing in the ADS divided by the total amount that has been loaded in the previous cycles. Figure A.3 depicts an integral view of the accumulated inventory that was loaded in the ADS along the successive cycles and the total amount that was transmuted. The figures clearly point out an almost asymptotic behaviour in the Pu-isotopes elimination, if the previous scheme is adopted. Of course, the ADS fuel becomes more and more ^{240}Pu dominated, which enables us to reconsider a second pattern of recycling. Instead of keeping the isotopic composition of the LWR-unloaded Pu, after reaching the equilibrium cycle in ADS, the successive cycles must be loaded with the isotopic

composition of the Pu discharged from the equilibrium cycle (i.e., there is a second phase that can be called ADS recycling). The isotopic composition was given before in Eq. (A.9)

Figure A.2 **Residual fraction of Pu isotopes for the case given in A.1**

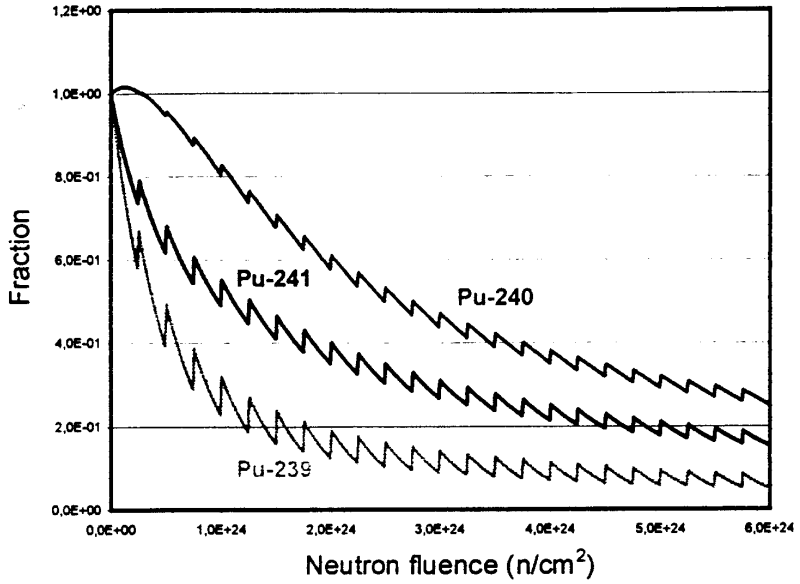

Figure A.4 shows the evolution of the residual fraction of the Pu-isotopes, as defined for figure A.2. Here, a third phase was set up after cycle 24, once the new isotopic composition (of Eq.(A.9)) reached again the equilibrium cycle. In this case, the isotopic composition of the discharged Pu is

$$^{239}\text{Pu} = 0.0962 \qquad ^{240}\text{Pu} = 0.7054 \qquad ^{241}\text{Pu} = 0.1984 \tag{A.10}$$

Of course, the very small amount of Pu-odd isotopes poses a problem about the quality of the fuel in order to get a high-enough k_{eff}. This problem disappears if it is considered that the ADS neutronics is mainly boosted by ^{233}U (albeit this isotopes poses a new problem, related to its own radiotoxicity along a very long time span, because its half-life is ~ 1.6×10^5 years).

Figure A.4 depicts that the residual fraction of ^{239}Pu reaches very low values, of the order of 0.1%, while ^{240}Pu arrives to ~ 15% and ^{241}Pu to ~ 13% (this one is mainly created by ^{240}Pu conversion). In fact, from the governing equations given in (A.3) through (A.8) and from the σ values given in (A.1) it is easily seen that it is possible to destroy ^{239}Pu, but it is difficult to get a high level of ^{240}Pu cleansing and therefore of ^{241}Pu elimination. If Eqs. (A.6) through (A.8) are solved for a continuous cycle without unloading-reloading, it is seen that the residual fraction of ^{239}Pu follows nearly the law

$$f_q = 10^{-x} \tag{A.11}$$

where $x = \phi t/10^{24}$. However, the residual fractions of ^{240}Pu and ^{241}Pu follows the law

$$f_{0,1} = 10^{-y} \tag{A.12}$$

with y = $\phi t/3\times10^{24}$. Hence, for $\phi t=6\times10^{24}$ (which is a very large value of fluence) the residual fraction of ^{239}Pu would be ~ 1 ppm, while the fraction of ^{240}Pu would be ~ 1.1% and that of ^{241}Pu ~ 0.8%.

Figure A.3 **Accumulated inventory loaded in the transmutator and total amount of transmuted material for the case given in A.1**

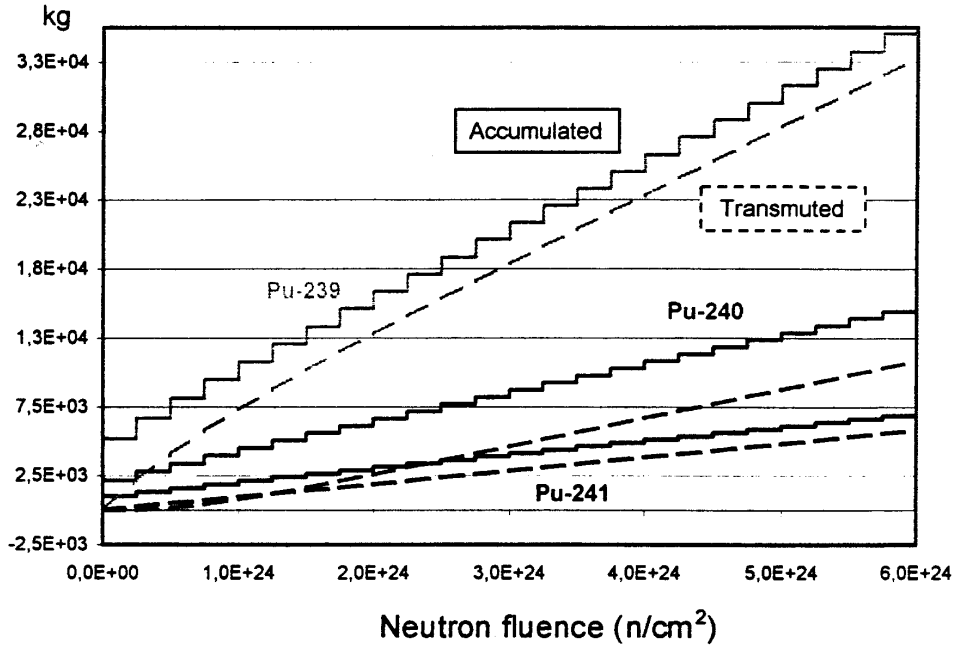

Figure A.4 **Accumulated inventory loaded in the transmutator and total amount of transmuted material for the case of using recycled fuel from the equilibrium cycles of the transmutator after 12 and 24 cycles**

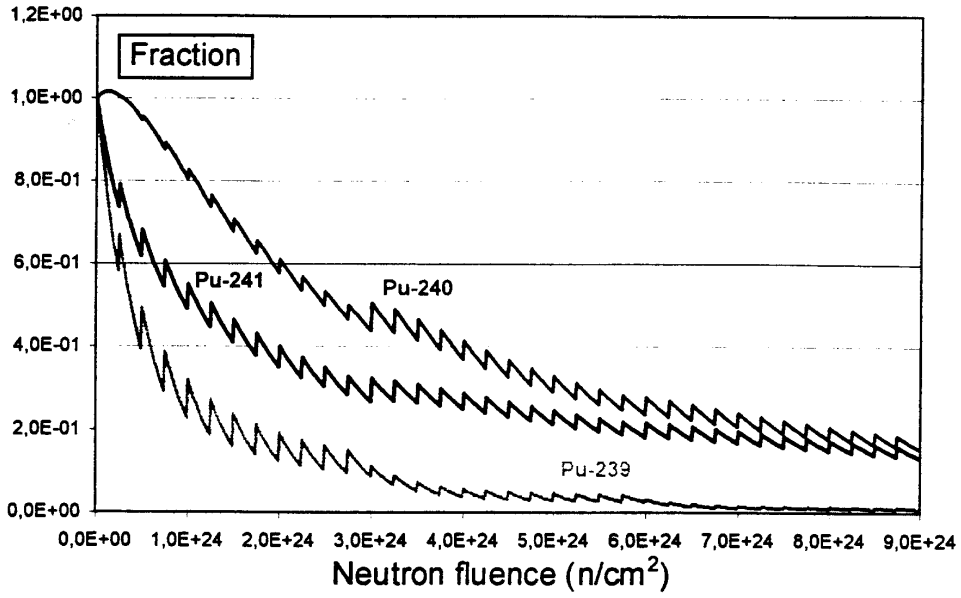

Acknowledgements

Research stay of A. Oda (from Kyushu University) in Madrid was supported by Japan's Ministry of Education, Science and Culture (JMESC) and by Spain's Foundation F^2I^2.

This work has been done in the framework of the ENRESA research contract 703275 for the study of Transmutation Efficiency of ADS.

REFERENCES

[1] C. Rubbia *et al,. Conceptual Design of a Fast Neutron Operated High Power Energy Amplifier*, CERN/AT/95-44(ET)(1995).

[2] C. Rubbia and J.A. Rubio, *A Tentative Programme Towards a Full Scale Energy Amplifier*, CERN/LHC/96-11 (ET)(1996).

[3] M. Piera, J.M. Martínez-Val, Kerntechnik, 50, 197 (1987).

[4] J.M. Martínez-Val *et al*, Nuclear Technology, 90, 371 (1990).

[5] Prael and H. Lichtenstein, *User Guide to LCS; The LAHET Code System*, Los Alamos National Laboratory report LA-UR-89-3014 (1989).

[6] J.F. Briesmeister, *MCNP™. A General Monte Carlo N-particle Transport Code*. LA-2625-M. Los Alamos National Laboratory Report (1993).

[7] M.K. Drake (edited) *Data Formats and procedures for the ENDF Neutron Cross Section Library*, BNL-50274(T-601, TID-4500), ENDF-102, Vol.1 (1970). Revised 1974.

[8] R.J. Howerton *et al*., *The LLL Evaluated Nuclear Data Library (ENDL): Evaluation Techniques, Reaction Index, and Description of individual Reactions*. Lawrence Livermore National Laboratory report UCRL-50400, Vol.15, Part A (1975).

[9] K. Kosako *et al*., *FSXLIB-J3R2: A Continuos Energy Cross Section Library for MCNP based on JENDL-3.2*, JAERI-Data/Code 94-020 (1994).

[10] A.Oda, J.M. Martínez-Val, M. Perlado *A Note on criticality studies on molten-lead Energy Amplifiers*, to appear in *Nuclear Technology*, December 1998.

[11] M. Segev, A. Galperin, *An estimation of the Energy Generation Potential of Proton-Driven Subcritical ThO_2 Lattices*, Nuc.Sci.Eng., 125, 84 (1997).

[12] M. Salvatores *et al*., *The potential of Accelerator-Driven Systems for transmutation of power production using Th or U fuel cycles*. Nuc.Sci.Eng., 126, 333 (1997).